

Reconstructions of the InP(111)A surface

C. H. Li, Y. Sun, D. C. Law, S. B. Visbeck, and R. F. Hicks*

Chemical Engineering Department, University of California, Los Angeles, California 90095, USA

(Received 20 August 2002; revised manuscript received 7 February 2003; published 21 August 2003)

Indium phosphide was deposited on InP(111)A substrates by metalorganic vapor-phase epitaxy. Then, the surface was characterized by scanning tunneling microscopy, low-energy electron diffraction, and x-ray photoelectron spectroscopy. Two reconstructions were observed: the (2×2) and the $(\sqrt{3} \times \sqrt{3})R30^\circ$ with phosphorus coverages of 0.25 and 1.00 ± 0.05 ML (monolayers), respectively. The (2×2) was found to adopt an indium-vacancy structure such as that observed on the (2×2) phase of GaAs (111)A. The $(\sqrt{3} \times \sqrt{3})R30^\circ$ reconstruction has not been seen previously on III/V semiconductor surfaces. The experimental evidence suggests that this surface is terminated with a complete layer of phosphorus trimers.

DOI: 10.1103/PhysRevB.68.085320

PACS number(s): 81.15.Gh, 81.05.Ea, 68.35.Bs, 68.37.Ef

I. INTRODUCTION

The (111) surfaces of cubic compound semiconductors are of interest for both scientific and technological reasons. Together with wurtzite GaN (0001), they form a family of surfaces in which one can investigate the nature of the chemical bonds formed between the group IIIA elements and nitrogen, phosphorus, and arsenic. On the technological side, it has been reported that strained heterostructures on GaAs and InP(111) exhibit inherent piezoelectric fields that may be exploited in several device applications.^{1,2} In addition, laser structures grown on (111) substrates have been shown to yield lower threshold currents than those grown on (001) substrates.³⁻⁵

The surface reconstructions of gallium arsenide (111) have been investigated by scanning tunneling microscopy,⁶⁻⁹ x-ray photoemission spectroscopy,^{9,10} electron-diffraction techniques,^{11,12} and total-energy calculations.^{13,14} The gallium-terminated (111)A surface forms a (2×2) lattice with one Ga vacancy in each unit cell. By contrast, the arsenic-terminated (111)B surface forms a (2×2) , $(\sqrt{19} \times \sqrt{19})$, and a (1×1) reconstruction with decreasing As coverage. The (2×2) reconstruction on the (111)B face is terminated with one As trimer per unit cell on top of a complete layer of As atoms.⁶ To our knowledge, no investigations have been made of the (111) surfaces of indium phosphide.

In this paper, we present a study of the atomic structure of InP(111)A using scanning tunneling microscopy (STM), low-energy electron diffraction (LEED), and x-ray photoelectron spectroscopy (XPS). Two reconstructions have been observed depending on the coverage, the (2×2) and the $(\sqrt{3} \times \sqrt{3})R30^\circ$. Atomic structures are proposed for both of these reconstructions that are consistent with the experimental results.

II. EXPERIMENTAL METHODS

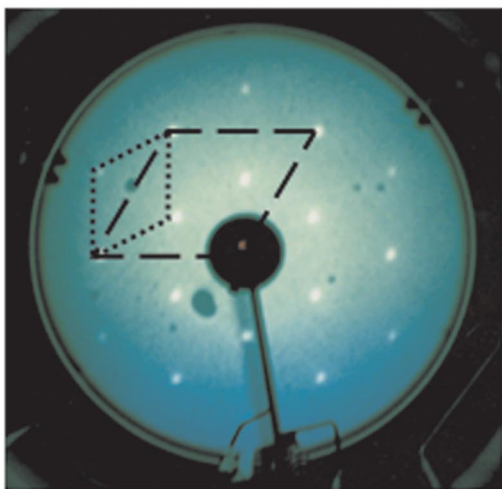
The experiments were conducted in an ultrahigh vacuum (UHV) surface analysis system interfaced to a metalorganic vapor-phase epitaxy (MOVPE) reactor.¹⁵ Single-crystal InP(111) films were deposited at 575 °C, 9.4×10^{-4} Torr trimethylindium, 0.12 Torr tertiarybutylphosphine, 20 Torr hy-

drogen, and a space velocity of 30 cm/s over the wafer surface (relative to 0 °C and 760 Torr). The H₂ carrier gas was passed through a SAES Gas hydrogen purifier to remove any remaining oxygen, nitrogen, and carbon containing impurities. The substrates were epi-ready InP(111) wafers (AXT, Inc., Fremont, CA) that were doped with 3×10^{18} S atoms/cm³. After growth, the crystals were cooled to 300 °C in tertiarybutylphosphine and hydrogen, and then to 150 °C in H₂ only. Finally, the samples were transferred to the UHV system through an interface chamber that was maintained at 10^{-8} Torr.

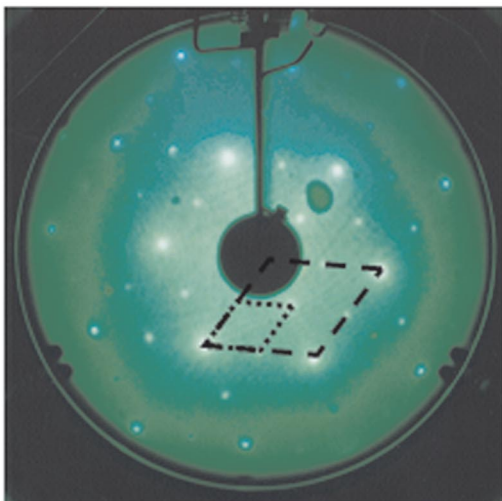
Once in vacuum, the InP crystals were annealed for 20 min at temperatures between 200 and 470 °C, and then cooled back down to 30 °C. The long-range order on the surface was characterized with a Princeton Instruments LEED. Then the chemical composition of the surface was determined by recording photoemission spectra of the P 2*p*, In 3*d*, C 1*s*, and O 1*s* lines using a Physical Electronics 3057 x-ray photoelectron spectrometer equipped with a hemispherical analyzer, multichannel detector, and Al K_α x-ray source. All XPS spectra were taken in small area mode with a 7° acceptance angle and 23.5 eV pass energy. A 25° take-off angle with respect to the surface normal was used. Finally, STM were obtained with a Park Scientific Autoprobe VP at a sample bias of +3.1 V and a tunneling current of 0.5 nA.

III. RESULTS

Two reconstructions were found on InP(111)A: the $(\sqrt{3} \times \sqrt{3})R30^\circ$ and the (2×2) . The LEED patterns observed for these structures are presented in Fig. 1. The overlayer pattern and the (1×1) spots are indicated by dotted and dashed parallelograms, respectively. Note that for the former structure, the reciprocal-space unit cell is $1/\sqrt{3}$ in length and rotated 30° with respect to the (1×1) . Both patterns exhibit sharp diffraction spots, indicating that the surfaces are well ordered. The $(\sqrt{3} \times \sqrt{3})R30^\circ$ was observed after removing the InP(111) crystal from the MOVPE reactor and annealing the sample for 20 min at 250 °C in vacuum. The (2×2) , on the other hand, was obtained by annealing the crystal for 20 min at 400 °C. Following heating at temperatures between 250 and 400 °C, the surfaces were found to contain mixtures



(a)



(b)

FIG. 1. Low-energy electron diffraction patterns recorded for the InP(111)A surface: (a) $(\sqrt{3} \times \sqrt{3})R30^\circ$ at 40 eV and (b) (2×2) at 80 eV.

of the $(\sqrt{3} \times \sqrt{3})R30^\circ$ and the (2×2) phases. If the (2×2) was exposed to 1×10^{-5} Torr phosphine for 15 min at 250°C , the surface would revert back to the $(\sqrt{3} \times \sqrt{3})R30^\circ$ reconstruction.

In Fig. 2, a large-scale scanning tunneling micrograph of the $(\sqrt{3} \times \sqrt{3})R30^\circ$ phase is presented. Three atomic layers can be seen separated by bilayer steps $3.5 \pm 0.3 \text{ \AA}$ in height. The top, middle, and bottom layers cover areas ranging from several hundred to several thousand square angstroms, indicating a two-dimensional growth mode. The island edges are kinked, but locally run along the $[110]$, $[011]$, and $[101]$ directions, consistent with the threefold symmetry of the (111). The roughness of the step edges varied from sample to sample with the slowest cooling rate producing the most kinks.

Shown in Fig. 3(a) is an atomic-resolution scanning tun-

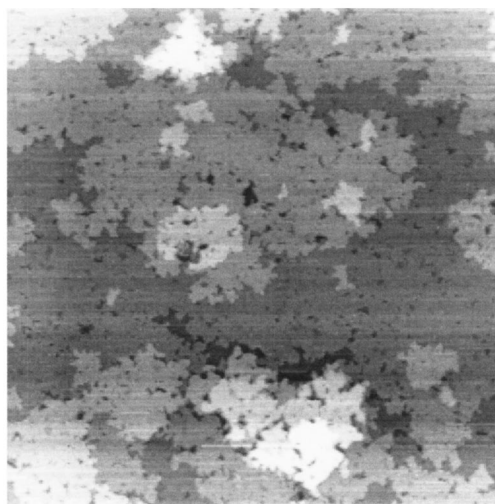


FIG. 2. Scanning tunneling micrograph of the $(\sqrt{3} \times \sqrt{3})R30^\circ$ surface (image size = $1.0 \times 1.0 \mu\text{m}^2$).

neling micrograph of the $(\sqrt{3} \times \sqrt{3})R30^\circ$ surface. This image was taken at a positive bias, probing the empty electronic states on the surface. Many attempts were made, but it was not possible to achieve stable tunneling at negative bias. In the figure, one sees a hexagonal pattern of gray spots with a distance between nearest neighbors of $7.0 \pm 0.3 \text{ \AA}$. This agrees with the $(\sqrt{3} \times \sqrt{3})$ periodicity recorded by LEED. One unit cell is highlighted in the smaller image with the white dashed parallelogram. Also present in the STM image are depressions that are randomly distributed over the surface

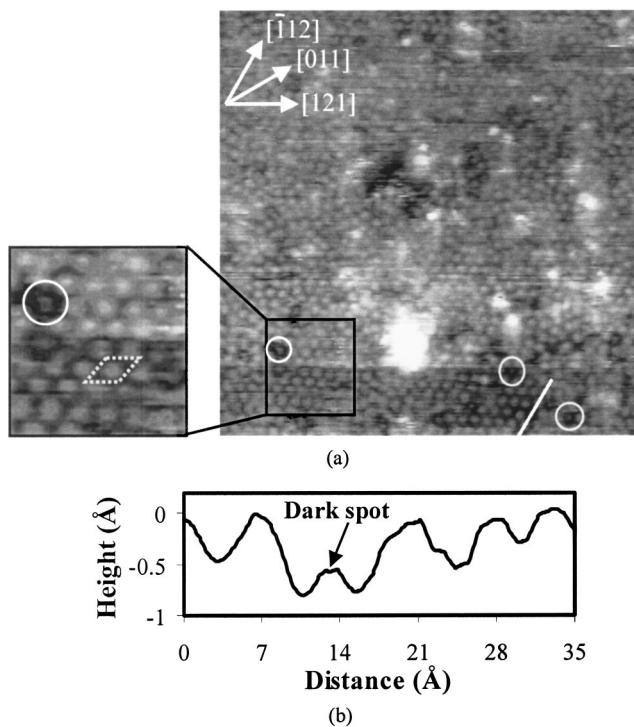


FIG. 3. (a) Atomic resolution image of the $(\sqrt{3} \times \sqrt{3})R30^\circ$ structure (image size = $216 \times 216 \text{ \AA}^2$, inset = $64 \times 64 \text{ \AA}^2$). (b) Line scan across five spots in (a) as indicated by white stripe.

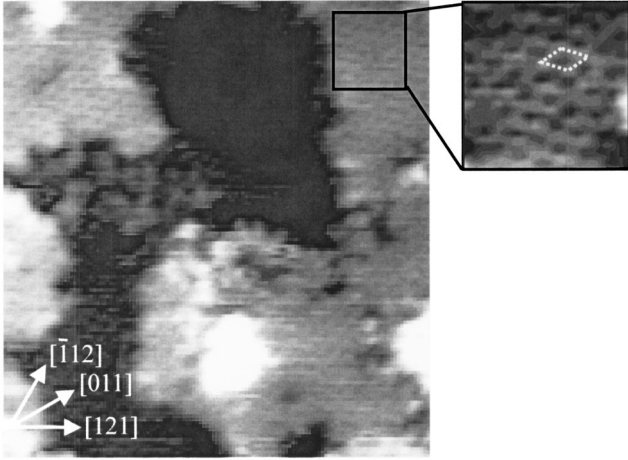


FIG. 4. Atomic resolution image of the (2×2) surface (image size = $216 \times 216 \text{ \AA}^2$, inset = $64 \times 64 \text{ \AA}^2$).

(three examples are circled). The coverage of these features is $\approx 3\%$.

Shown in Fig. 3(b) is a line scan through five of the gray spots on the surface, corresponding to the white line in the STM picture. The corrugation from the bottom to the top of the spots averages $0.4 \pm 0.1 \text{ \AA}$, which is much less than the atomic layer height of InP(111)A, i.e., 1.7 \AA . One of the dark spots has also been scanned and it appears 0.6 \AA lower than its neighbors. This difference in height suggests that these depressions are not due to vacancies, but rather to impurity atoms or adsorbates.

An empty-states scanning tunneling micrograph of the (2×2) phase is presented in Fig. 4. Three bilayers of the surface are seen in this picture. The contrast has been increased to reveal the reconstruction on the middle terrace. The magnified image on the right shows the (2×2) pattern of gray and black spots. One of the unit cells is highlighted with white dashed lines. The length along the edge of the unit cell is $8.1 \pm 0.3 \text{ \AA}$. Within this distance, one can discern a row of three gray spots, although the resolution is not high enough to clearly resolve these features. The image presented in the figure is basically the same as that seen for the (2×2) reconstruction on GaAs (111)A.^{8,9}

Shown in Table I are the normalized indium and phosphorus compositions of the $(\sqrt{3} \times \sqrt{3})R30^\circ$ and (2×2) surfaces obtained by excluding the contributions from carbon and oxygen. The concentration of these impurities was less than 10.0 and 2.0 at.%, respectively. As the structure changes from $(\sqrt{3} \times \sqrt{3})R30^\circ$ to (2×2) , the atomic concentration of phosphorus falls from 42.7% to 37.8% with a standard deviation of $\pm 1.0\%$. Also shown in the table for comparison are the XPS results recorded for the InP(001) (2×1) and $\delta(2 \times 4)$ phases.¹⁶ Note that the atomic concentration of phosphorus on the $(\sqrt{3} \times \sqrt{3})R30^\circ$ is the same as that on the (2×1) . On the other hand, the P atomic percent on the (2×2) is higher than that on the $\delta(2 \times 4)$.

The phosphorus coverage on the (111) surface can be determined from a quantitative analysis of the XPS data. The photoemission process is described by the following equation:¹⁷⁻¹⁹

TABLE I. Normalized In and P composition for InP surfaces.

Surface	Structure	Atomic percent		Phosphorus Coverage (ML)
		In	P	
InP(111)A	$(\sqrt{3} \times \sqrt{3})R30^\circ$	57.3	42.7	1.00
	(2×2)	62.7	37.3	0.25
InP(001)	(2×1)	57.5	42.5	1.00
	$\delta(2 \times 4)$	63.4	36.6	0.13

$$I_p \propto \exp\left(\frac{-l}{\lambda \cos \alpha}\right), \quad (1)$$

where I_p is the P $2p$ peak intensity for the InP surface, l is the distance from the surface into the bulk, λ is the P $2p$ photoelectron inelastic mean free path, which equals 26 \AA ,²⁰ and α is the take-off angle, 25° . The normalized intensity of the P $2p$ photoemission line for InP is

$$I_{P/\text{InP}} = (N_P/N_T) \exp\left(\frac{-l}{\lambda \cos \alpha}\right). \quad (2)$$

Here, N_T and N_P are the total atom and phosphorus atom concentrations per centimeter cube, respectively. An analogous expression can be derived for indium, knowing that the λ of the In $3d$ photoelectrons is 24 \AA .²⁰

To calculate the phosphorus atomic percentage, one has

$$P(\text{atomic percentage}) = \frac{\int_0^\infty N_P \times \exp\left(\frac{-l}{\lambda \cos \alpha}\right) dl}{N_T \int_0^\infty \exp\left(\frac{-l}{\lambda \cos \alpha}\right) dl}. \quad (3)$$

This equation may be solved by summing the expressions inside the integrands over the first 20 atomic layers of the film or about 35 \AA . On an InP(111)A sample, the only variable is the first atomic layer, while the rest of the 20 bulk layers remain the same. The phosphorus coverage appears in the value of N_P for the first atomic layer. Consequently, Eq. (3) yields a nearly linear dependence of the P atomic percent on the phosphorus coverage. It should be noted that the first atomic layer accounts for only 19.1% and 20.2% of the measured P $2p$ intensities for the InP(001) and (111)A surfaces, respectively. Using the XPS data for InP(001) to calibrate the phosphorus coverage, we obtain a P coverage of $1.0 \pm 0.05 \text{ ML}$ (monolayers) on the $(\sqrt{3} \times \sqrt{3})R30^\circ$ and $0.25 \pm 0.05 \text{ ML}$ on the (2×2) . These results are tabulated in the last column of Table I.

IV. DISCUSSION

The In-rich (2×2) observed for InP(111)A most likely exhibits the same vacancy structure that has been proposed for the Ga-rich (2×2) on GaAs (111)A.^{8,9} A model of this reconstruction is presented in Fig. 5. One indium atom is missing in every (2×2) unit cell, yielding an In coverage of 0.75 ML . The top layer indium atoms each have an empty

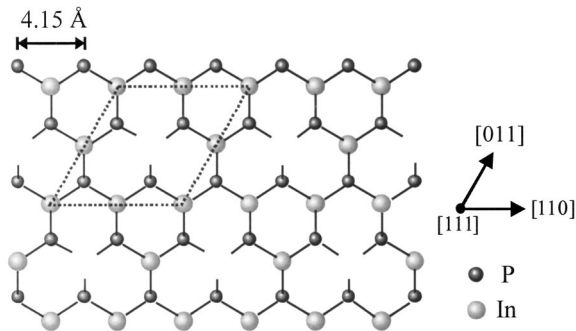


FIG. 5. The indium vacancy model for the (2×2) reconstruction.

dangling bond, which is consistent with the pattern of gray spots seen in the empty-states scanning tunneling micrographs.^{8,9} Furthermore, total-energy calculations indicate that this structure is the most stable configuration for the group III-rich surfaces.^{13,14}

For the As-rich GaAs (111)A surface, it has been proposed that a (2×2) reconstruction should be observed which is terminated with arsenic trimers.^{13,14} This model is presented in Fig. 6(a). Each unit cell contains one As trimer and one exposed Ga atom in the second layer with an empty dangling bond. The arsenic coverage is 0.75 ML. Kaxiras and co-workers¹³ calculated that this surface is 1.7 eV more stable in energy than other possible As-rich reconstructions of GaAs (111)A. It was therefore somewhat surprising to them that the arsenic trimer reconstruction was not recorded in the experiments.⁶⁻¹²

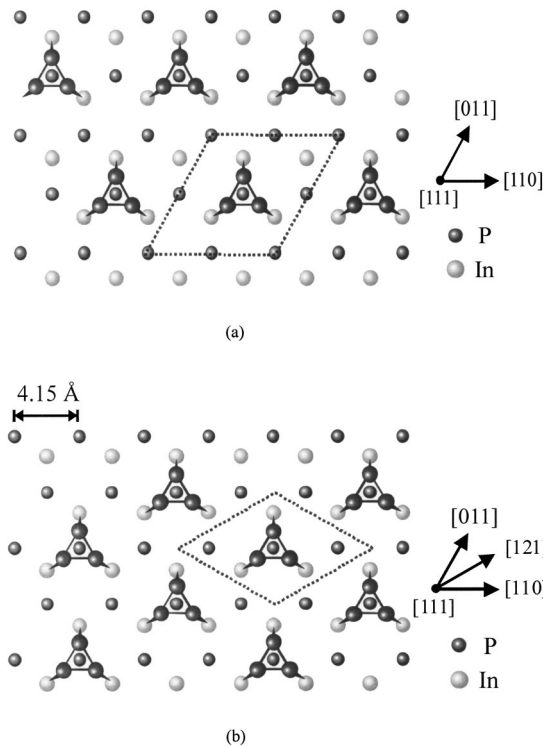


FIG. 6. (a) The arsenic trimer model for the (2×2) GaAs (111)A surface (Ref. 13). (b) The phosphorus trimer model for the $(\sqrt{3} \times \sqrt{3})R30^\circ$ InP(111)A surface.

On InP(111)A, we observe a $(\sqrt{3} \times \sqrt{3})R30^\circ$ reconstruction with a phosphorus coverage of 1.00 ML. A model for this phase is proposed in Fig. 6(b). It is based on Kaxiras' structure [Fig. 6(a)], with the only difference being that the phosphorus trimers are closest packed, i.e., every second-layer In atom is fourfold coordinated. The proposed structure is consistent with the STM picture in Fig. 3. The gray spots associated with each phosphorus trimer exhibit a hexagonal arrangement with a separation of 7.0 Å. Moreover, the corrugation measured in the image is only 0.4 ± 0.1 Å, indicating that it is unlikely for any lower layer indium atoms to be exposed on this surface. To be consistent with the models proposed for GaAs (111), the phosphorus trimers have been placed at the T_4 sites, i.e., directly above the third-layer P atoms.^{6,13,14}

As Kaxiras and co-workers^{13,14} pointed out, the group V trimer is very stable on the (111)A surface, resulting in only a minor distortion of the surface charge density. Nearly vertical bonds are formed between the In and P atoms, yielding the preferred sp^3 hybridization with minimal compressive stress on the underlying layer. Evidently, the InP(111)A surface forms the $(\sqrt{3} \times \sqrt{3})$ trimer over the (2×2) trimer so that it can accommodate 33% more P-P bonds. These bonds are quite strong, with energies of ≈ 5 eV.²² Moreover, the phosphorus-rich growth conditions used in the MOVPE reactor would tend to favor a higher packing density of the trimers on the indium phosphide surface.

The $(\sqrt{3} \times \sqrt{3})R30^\circ$ P-trimer structure does not follow the electron counting rule presented by Pashley twelve years ago.²¹ Each phosphorus atom contributes $\frac{5}{4}$ electrons to the indium back bonds and two electrons to the two P-P bonds of the trimer. Thus, each phosphorus dangling bond is left with $\frac{7}{4}$ electrons. In order to completely fill the phosphorus dangling bonds, it is necessary to spread the trimers apart, creating a (2×2) reconstruction with a trimer and an empty group III dangling bond in every unit cell [cf., Fig. 6(a)]. However, this is not the structure observed. Although the proposed trimer structure for the $(\sqrt{3} \times \sqrt{3})R30^\circ$ does not obey the electron counting model, this is not sufficient reason for ruling it out. There are several examples in the literature of compound semiconductor surfaces having partially filled dangling bonds.²³⁻²⁶

One possible way to fill the phosphorus dangling bonds is to adsorb three hydrogen atoms onto every four $(\sqrt{3} \times \sqrt{3})$ unit cells. This would be similar to the structure that has been recently proposed for the phosphorus-rich InP(001) surface.²⁷ Here a (2×1) reconstruction is observed in which the surface is covered with a complete monolayer of phosphorus dimers.^{28,29} In order to obey the electron counting model, every other P atom should be bonded to an H atom.²⁷ While we cannot rule out the presence of hydrogen on the InP(111)A surface, one would expect the adsorbed H atoms to alter the LEED pattern or the STM image in some discernable way. No evidence for this can be seen in the experimental data. The dark spots in the STM image are at 3% coverage, well below the 25% H coverage needed to saturate the P dangling bonds. Nevertheless, further work should be done to explore whether hydrogen is adsorbed onto the $(\sqrt{3} \times \sqrt{3})R30^\circ$ reconstruction.

In summary, we have observed two stable reconstructions on the InP(111)A surface: the (2×2) and the $(\sqrt{3} \times \sqrt{3})R30^\circ$ with phosphorus coverages of 0.25 and 1.00 ± 0.05 ML, respectively. The former structure contains one indium vacancy per unit cell, while the latter structure is most likely terminated with a complete layer of phosphorus trimers.

ACKNOWLEDGMENTS

Funding for this research was provided by the National Science Foundation, Divisions of Chemical and Transport Systems and Materials Research, TRW Inc., Epichem Inc., Emcore Corp., and the UC-SMART program.

*Author to whom correspondence should be addressed. Email address: rhicks@ucla.edu

- ¹E. A. Caridi, T. Y. Chang, K. W. Goosen, and L. F. Eastman, *Appl. Phys. Lett.* **56**, 659 (1990).
- ²D. L. Smith, *Solid State Commun.* **57**, 919 (1986); D. L. Smith and C. Mailhot, *J. Appl. Phys.* **63**, 2717 (1988).
- ³Y. Kajikawa, N. Sugiyama, T. Kamijoh, and Y. Katayama, *Jpn. J. Appl. Phys., Part 2* **28**, L1022 (1989).
- ⁴D. L. Smith and C. Mailhot, *Phys. Rev. Lett.* **58**, 1264 (1987).
- ⁵T. Hayakawa, T. Suyama, K. Takashashi, M. Kondo, S. Yamamoto, and T. Hijikata, *Appl. Phys. Lett.* **52**, 339 (1988).
- ⁶D. K. Biegelsen, R. D. Bringans, J. E. Northrup, and L.-E. Swartz, *Phys. Rev. Lett.* **65**, 452 (1990).
- ⁷J. M. C. Thornton, D. A. Woolf, and P. Weightman, *Surf. Sci.* **380**, 548 (1997).
- ⁸K. W. Haberern and M. D. Pashley, *Phys. Rev. B* **41**, 3226 (1990).
- ⁹J. M. C. Thornton, P. Weightman, D. A. Woolf, and C. J. Duncombe, *Phys. Rev. B* **51**, 14459 (1995).
- ¹⁰J. M. C. Thornton, P. Weightman, D. A. Woolf, and C. J. Duncombe, *J. Electron Spectrosc. Relat. Phenom.* **72**, 65 (1995).
- ¹¹S. Y. Tong, G. Xu, and W. N. Mei, *Phys. Rev. Lett.* **52**, 1693 (1984).
- ¹²J. Bohr, R. Feidenhans'l, M. Neilsen, M. Toney, R. L. Johnson, and I. K. Robinson, *Phys. Rev. Lett.* **54**, 1275 (1985).
- ¹³E. Kaxiras, Y. Bar-Yam, J. D. Joannopoulos, and K. D. Pandey, *Phys. Rev. B* **35**, 9625 (1987).
- ¹⁴E. Kaxiras, Y. Bar-Yam, J. D. Joannopoulos, and K. D. Pandey, *Phys. Rev. B* **35**, 9636 (1987).
- ¹⁵L. Li, B.-K. Han, S. Gan, H. Qi, and R. F. Hicks, *Surf. Sci.* **398**, 386 (1998).
- ¹⁶D. C. Law, Y. Sun, C. H. Li, G. Chen, S. B. Visbeck, and R. F. Hicks, *Phys. Rev. B* **66**, 045314 (2002).
- ¹⁷L. C. Feldman and J. W. Mayer, *Fundamentals of Surface and Thin Film Analysis* (Elsevier Science, New York, 1986).
- ¹⁸Y. Feurprier, Ch. Cardinaud, and G. Turban, *J. Vac. Sci. Technol. B* **16**, 1823 (1998).
- ¹⁹V. I. Nefedov, *X-ray Photoelectron Spectroscopy of Solid Surfaces* (VSP BV, Utrecht, 1988).
- ²⁰C. J. Powell (private communication).
- ²¹M. D. Pashley, *Phys. Rev. B* **40**, 10 481 (1989).
- ²²J. A. Dean, *Lange's Handbook of Chemistry*, 15th ed. (McGraw-Hill, New York, 1999).
- ²³A. R. Smith, R. M. Feenstra, D. W. Greve, M. S. Shin, M. Skowronski, J. Neugebauer, and J. E. Northrup, *J. Vac. Sci. Technol. B* **16**, 2242 (1998).
- ²⁴J. E. Northrup and J. Neugebauer, *Phys. Rev. B* **57**, R4230 (1998).
- ²⁵L. J. Whitman, P. M. Thibado, S. C. Erwin, B. R. Bennett, and B. V. Shanabrook, *Phys. Rev. Lett.* **79**, 693 (1997).
- ²⁶P. M. Thibado, B. R. Bennett, B. V. Shanabrook, and L. J. Whitman, *J. Cryst. Growth* **175**, 317 (1997).
- ²⁷W. G. Schmidt, P. H. Hahn, F. Bechstedt, N. Esser, P. Vogt, A. Wange, and W. Richter, *Phys. Rev. Lett.* **90**, 126101 (2003).
- ²⁸L. Li, B.-K. Han, Q. Fu, and R. F. Hicks, *Phys. Rev. Lett.* **82**, 1879 (1999).
- ²⁹Q. Fu, E. Negro, G. Chen, C. H. Li, D. C. Law, R. F. Hicks, and K. Raghavachari, *Phys. Rev. B* **65**, 75318 (2002).